



1 **Not all feldspar is equal: a survey of ice nucleating**
2 **properties across the feldspar group of minerals**

3

4 **Alexander D. Harrison^{1‡}, Thomas F. Whale^{1‡*}, Michael A. Carpenter², Mark A.**
5 **Holden¹, Lesley Neve¹, Daniel O'Sullivan¹, Jesus Vergara Temprado¹, Benjamin**
6 **J. Murray^{1*}**

7 ¹School of Earth and Environment, University of Leeds, Leeds, LS2 9JT, UK

8 ² Department of Earth Sciences, University of Cambridge, Downing Street, Cambridge CB2
9 3EQ, UK

10 Correspondence to: T. F. Whale (t.f.whale@leeds.ac.uk) and B. J. Murray
11 (b.j.murray@leeds.ac.uk)

12

13 [‡] Both authors contributed equally to the paper

14

15 **Abstract**

16 Mineral dust particles from wind-blown soils are known to act as effective ice nucleating
17 particles in the atmosphere and are thought to play an important role in the glaciation of
18 mixed phase clouds. Recent work suggests that feldspars are the most efficient nucleators of
19 the minerals commonly present in atmospheric mineral dust. However, the feldspar group of
20 minerals is complex, encompassing a range of chemical compositions and crystal structures.
21 To further investigate the ice-nucleating properties of the feldspar group we measured the ice
22 nucleation activities of 15 well-characterised feldspar samples. We show that alkali feldspars,
23 in particular the potassium feldspars, generally nucleate ice more efficiently than feldspars
24 containing significant amounts of calcium in the plagioclase series. We also find that there is
25 variability in ice nucleating ability within these groups. While five out of six potassium-rich
26 feldspars have a similar ice nucleating ability, one potassium rich feldspar sample and one
27 sodium-rich feldspar sample were significantly more active. The hyper-active Na-feldspar
28 was found to lose activity with time suspended in water with a decrease in mean freezing
29 temperature of about 16°C over 16 months; the mean freezing temperature of the hyper-
30 active K-feldspar decreased by 2°C over 16 months, whereas the 'standard' K-feldspar did



1 not change activity within the uncertainty of the experiment. These results, in combination
2 with a review of the available literature data, are consistent with the previous findings that
3 potassium feldspars are important components of soil dusts for ice nucleation. However, we
4 also show that there is the possibility that some alkali feldspars can have enhanced ice
5 nucleating abilities, which could have implications for prediction of ice nucleating particle
6 concentrations in the atmosphere.

7

8 **1 Introduction**

9 Clouds containing supercooled liquid water play an important role in our planet's climate and
10 hydrological cycle, but the formation of ice in these clouds remains poorly understood
11 (Hoose and Möhler, 2012). Cloud droplets can supercool to below -35°C in the absence of
12 particles capable of nucleating ice (Riechers et al., 2013; Herbert et al., 2015), hence clouds
13 are sensitive to the presence of ice nucleating particles (INPs). A variety of aerosol types
14 have been identified as INPs (Murray et al., 2012; Hoose and Möhler, 2012), but mineral
15 dusts from deserts are thought to be important INPs over much of the globe and in a variety
16 of cloud types (Atkinson et al., 2013; DeMott et al., 2003; Hoose et al., 2010; Hoose et al.,
17 2008; Niemand et al., 2012).

18 Atmospheric mineral dusts are composed of weathered mineral particles from rocks and soils,
19 and are predominantly emitted to the atmosphere in arid regions such as the Sahara (Ginoux
20 et al., 2012). The composition and relative concentrations of dust varies spatially and
21 temporally but it is generally made up of only a handful of dominant minerals. The most
22 common components of dust reflect the composition of the continental crust and soil cover,
23 with clay minerals, feldspars and quartz being major constituents. Until recently, major
24 emphasis for research has been placed on the most common minerals in transported
25 atmospheric dusts, the clays. It has now been shown that, when immersed in water, the
26 feldspar component nucleates ice much more efficiently than the other main minerals that
27 make up typical desert dust (Augustin-Bauditz et al., 2014; O'Sullivan et al., 2014; Atkinson
28 et al., 2013; Niedermeier et al., 2015; Zolles et al., 2015). While all available evidence
29 indicates that feldspars are very effective INPs, it must also be recognised that feldspars are a
30 group of minerals with differing compositions and crystal structures. Therefore, in this study
31 we examine ice nucleation by a range of feldspar samples under conditions pertinent to mixed
32 phase clouds.



1 An additional motivation is that determining the nature of nucleation sites is of significant
2 fundamental mechanistic interest and is likely to help with further understanding of ice
3 nucleation in the atmosphere (Vali, 2014; Freedman, 2015; Slater et al., 2015). By
4 characterising a range of feldspars and associating them with differences in ice nucleation
5 activity it might be possible to build understanding of the ice nucleation sites on feldspars.
6 Some work has been conducted in this area already. Augustin-Bauditz et al. (2014) concluded
7 that microcline nucleates ice more efficiently than orthoclase on the basis of ice nucleation
8 results looking at a microcline feldspar and several mixed dusts. Zolles et al. (2015) recently
9 found that a plagioclase and an albite feldspar nucleated ice less well than a potassium
10 feldspar and suggested that the difference in the ice nucleation activity of these feldspars is
11 related to the difference in ionic radii of the cations and the local chemical configuration at
12 the surface. They suggested that only potassium feldspar will nucleate ice efficiently because
13 the K^+ is kosmotropic (structure making) in the water hydration shell while Ca^{2+} and Na^+ are
14 chaotropic (structure breaking).

15 There has been much interest in the study of ice nucleation using molecular dynamics
16 simulations e.g. (Cox et al., 2015a, b; Cox et al., 2012; Hu and Michaelides, 2007; Fitzner et
17 al., 2015; Reinhardt and Doye, 2014; Lupi and Molinero, 2014; Lupi et al., 2014; Zielke et
18 al., 2015). To date there has been little overlap between work of this nature and laboratory
19 experiment. This has been due to difficulties in conducting experiments on similar timescales
20 and spatial extents between real-world and computational systems. While these obstacles are
21 likely to remain in place for some time, the feldspars may offer the opportunity to address
22 this deficit by providing qualitative corroboration between computational and laboratory
23 results. For instance, it may be possible to study ice nucleation on different types of feldspar
24 computationally. If differences in nucleation rate observed also occur in the laboratory
25 greater weight may be placed on mechanisms determined by such studies and so a
26 mechanistic understanding of ice nucleation may be built up.

27 In this paper we have surveyed 15 feldspar samples with varying composition for their ice
28 nucleating ability. It will be shown that feldspars rich in alkali metal cations tend to be much
29 better at nucleating ice than those rich in calcium. First, we introduce the feldspar group of
30 minerals.

31

32



1 2 **The feldspar group of minerals**

2 The feldspars are tectosilicates (also called framework silicates) with a general formula of
3 $XAl(Si,Al)Si_2O_8$, where X is usually potassium, sodium or calcium (Deer et al., 1992).
4 Unlike clays, which are phyllosilicates (or sheet silicates), tectosilicates are made up of three
5 dimensional frameworks of silica tetrahedra. Substitution of Si with Al in the structure is
6 charge balanced by cation addition or replacement within the cavities in the framework. This
7 leads to a large variability of composition in the feldspars and means that most feldspars in
8 rocks have compositions between end-members of sodium-, calcium- or potassium-feldspars
9 (Wenk and Bulakh, 2004; Deer et al., 1992). A ternary representation of feldspar
10 compositions is shown in Figure 1. All feldspars have very similar crystal structures, but the
11 presence of different ions and degrees of disorder related to the conditions under which they
12 crystallised from the melt (lava or magma) yields subtle differences which can result in
13 differing symmetry.

14 There are three polymorphs (minerals with the same composition, but different crystal
15 structure) of the potassium end-member, which are microcline, orthoclase and sanidine. The
16 polymorphs become more disordered in terms of Al placement in the tetrahedra from
17 microcline to sanidine, respectively. The structures of feldspars which form from a melt vary
18 according to their cooling rate. If cooling is fast (volcanic), sanidine is preserved. If cooling is
19 slow, in some granites for example, microcline may be formed. Feldspars formed in
20 metamorphic rocks have high degrees of Al/Si order. The sodium end-member of the
21 feldspars is albite and the calcium end-member is anorthite. Feldspars with compositions
22 between sodium and calcium form a solid solution and are collectively termed the plagioclase
23 feldspars with specific names for different composition ranges. Feldspars between sodium
24 and potassium end-members are collectively termed the alkali feldspars and can be
25 structurally complex. A solid solution series exists between high albite and sanidine ('high'
26 refers to high temperature character which is preserved on fast cooling), but not between low
27 albite and microcline ('low' refers to low temperature character which is indicative of slow
28 cooling rates). In contrast to the series between sodium and calcium, and sodium and
29 potassium, there are no feldspars between calcium and potassium end-members because
30 calcium and potassium ions do not actively substitute for one another within the framework
31 lattice due their difference in size and ionic charge (Wenk and Bulakh, 2004; Deer et al.,
32 1992).



1 There is limited information about the composition of airborne atmospheric mineral dusts and
2 where mineralogy is reported the breakdown of the feldspar family has only been done in a
3 limited way. Atkinson et al. (2013) compiled the available measurements and grouped them
4 into K-feldspars and plagioclase feldspars (see the Supplementary Table 1 in Atkinson et al.
5 (2013)). This compilation indicates that the feldspar type is highly variable in atmospheric
6 dusts, with K-feldspars ranging from 1 to 25% by mass (with a mean of 5%) and plagioclase
7 feldspars ranging from 1 to 14% (with a mean of 7%). The feldspar component of airborne
8 soil dusts is highly variable and the nucleating ability of the various components needs to be
9 investigated.

10 In order to aid the discussion and representation of the data we have grouped the feldspars
11 into three groups: the plagioclase feldspars (not including albite), albite (the sodium rich
12 corner of the ternary diagram) and potassium (K-) feldspars (microcline, sanidine and
13 orthoclase). The K-feldspars contain varying amounts of sodium, but their naming is
14 determined by their crystal structure. We also collectively refer to albite and potassium
15 feldspars as alkali feldspars.

16

17 **3 Samples and sample preparation**

18 A total of 15 feldspars were sourced for this study. Details of the plagioclase feldspars tested
19 are in Table 1 and details of the alkali feldspars are in Table 2. We have made use of a series
20 of well characterised plagioclase feldspars which were assembled for previous studies
21 (Carpenter, 1991; Carpenter, 1986; Carpenter et al., 1985). The other samples were sourced
22 from a range of repositories, detailed in Tables 1 and 2. The naming convention we have used
23 in this paper is to state the identifier of the specific sample followed by the mineral name.
24 For example, BCS 376 microcline is a microcline sample from the Bureau of Analysed
25 Samples with sample code 376. In other cases, such as Amelia Albite, the sample is from a
26 traceable source and is commonly referred to with this name and when a code is used, such as
27 97490 plagioclase, the code links to the cited publications.

28 The anorthite glass tested was produced by Carpenter (1991) by melting natural calcite with
29 reagent grade SiO_2 and Al_2O_3 at 1680°C for 3 hours. The melt was then stirred before air
30 cooling. The resulting glass was then annealed at 800°C to relieve internal stresses. The



1 composition of the resulting glass was shown to be stoichiometric $\text{CaAl}_2\text{Si}_2\text{O}_8$. Synthetic
2 anorthite ANC 68 was produced by heating a sample of this glass to 1400°C for 170 hours.
3 Feldspars 148559, 21704a, 67796b and 97490 plagioclase and Amelia albite are natural
4 samples that form a solid solution series covering the plagioclase series from nearly pure
5 anorthite to nearly pure albite as seen in Table 1.

6 The alkali feldspars used here have not previously been characterised. Rietveld refinement of
7 powder XRD patterns was carried out using TOtal Pattern Analysis Solutions (TOPAS) to
8 determine the phase of the feldspar present. The results of this process are presented in Table
9 2. The surface areas of all the feldspars were measured by Brunauer-Emmett-Teller (BET)
10 nitrogen gas adsorption (see Sect. 4). All samples, unless otherwise stated, were ground to
11 reduce the particle size and increase the specific surface area using a mortar and pestle which
12 was scrubbed with pure quartz then cleaned with deionised water and methanol before use.
13 Grinding of most samples was necessary in order to make the particles small enough for our
14 experiments. Amelia albite was the only material tested both in an unground state (or at least
15 not a freshly ground state) and a freshly ground state. Suspensions of known concentration
16 were made up gravimetrically using Milli-Q water ($18.2 \text{ M}\Omega\cdot\text{cm}$). Except where stated
17 otherwise the suspensions were then mixed for a few minutes using magnetic stirrers prior to
18 use in ice nucleation experiments.

19 Three samples, the BCS 376 microcline, ground Amelia albite and TUD #3 microcline, were
20 tested for changes in ice nucleating efficiency with time, when left in suspension at room
21 temperature. Ice nucleation efficiency was quantified at intervals over 11 days. Between
22 experiments the suspensions were left at room temperature without stirring and then stirred to
23 re-suspend the particulates for the ice nucleation experiments. Suspensions of the three dusts
24 were also tested 16 months after initial experiments were performed to determine the long
25 term impact of contact with water on ice nucleation efficiency.

26

27 **4 Experimental method and data analysis**

28 In order to quantify the efficiency with which a range of feldspar dusts nucleate ice we made
29 use of the microliter Nucleation by Immersed Particle Instrument ($\mu\text{l-NIPI}$). This system has
30 been used to make numerous ice nucleation measurements in the past (O'Sullivan et al., 2015;
31 Hiranuma et al., 2015; Whale et al., 2015b; Herbert et al., 2014; O'Sullivan et al., 2014;



1 Atkinson et al., 2013; Umo et al., 2015; Wilson et al., 2015) and has been described in detail
2 by Whale et al. (2015a). Briefly, droplets of an aqueous suspension, containing a known
3 quantity of feldspar particles are pipetted onto a hydrophobic coated glass slide. This slide is
4 placed on a temperature controlled stage and cooled from room temperature at a rate of 5
5 °Cmin⁻¹ to 0 °C and then at 1 °Cmin⁻¹ until all droplets are frozen. Dry nitrogen is flowed over
6 the droplets at 0.2 l min⁻¹ to prevent frozen droplets from affecting neighbouring liquid
7 droplets. Freezing is observed with a digital camera, allowing determination of the fraction of
8 droplets frozen as a function of temperature. Multiple experiments have been combined to
9 produce single sets of data for each mineral. Suspensions of the feldspars were made up
10 gravimetrically and specific surface areas of the samples were measured using the Brunauer–
11 Emmett–Teller (BET) N₂ adsorption method using a Micromeritics TriStar 3000.

12 To normalise to surface area and allow comparison of different nucleators $n_s(T)$ values are
13 calculated. $n_s(T)$ is the number of ice nucleating sites that become active per surface area on
14 cooling from 0°C to temperature T . $n_s(T)$ can be calculated using (Connolly et al., 2009):

$$15 \quad \frac{n(T)}{N} = 1 - \exp(-n_s(T)A) \quad (1)$$

16 Where $n(T)$ is the number of droplets frozen at temperature T , N is the total number of
17 droplets in the experiment and A is the surface area of nucleator per droplet. This description
18 is site specific and does not include time dependence. The role of time dependence in ice
19 nucleation has recently been extensively discussed (Herbert et al., 2014; Vali, 2014). For
20 feldspar it is thought that the time dependence of nucleation is relatively weak (at least for
21 BCS 376 microcline) and that the particle to particle, or active site to active site, variability is
22 much more important.

23 In order to estimate the uncertainty in $n_s(T)$ due to the randomness of the distribution of the
24 active sites in droplet freezing experiments, we conducted Monte Carlo simulations. In these
25 simulations, we generate a list of possible values for the number of active sites per droplet
26 (k). The theoretical relationship between the fraction of droplets frozen and k can be derived
27 from the Poisson distribution:

$$28 \quad \frac{n(T)}{N} = 1 - \exp(-k) \quad (2)$$

29 and we can calculate $n_s(T)$ using the following:



1
$$n_s = \frac{k}{A} \tag{3}$$

2 The simulation works in the following manner. First, we take a value of k and we simulate a
3 corresponding random distribution of active sites through the droplet population for an
4 experiment. Every droplet containing one or more active sites is then considered to be frozen.
5 In this way, we can obtain a simulated value of the fraction frozen for a certain value of k .
6 Repeating this process many times and for all the possible values of k , we obtain a
7 distribution of possible values of k that can explain every value of the observed fraction
8 frozen. This resulting distribution is neither Gaussian nor symmetric, so in order to propagate
9 the uncertainty in Equation 3, we take the following steps. First, we generate random values
10 of k following the corresponding previously simulated distribution for every value of the
11 fraction frozen. Then, we simulate random values of A following a Gaussian distribution
12 centred on the value derived from the specific surface area per droplet with the standard
13 deviation derived from the uncertainty in droplet volume and specific surface area. We
14 assume that each droplet contains a representative surface area distribution. By combining
15 these two distributions of simulated values, we calculate the distribution of $n_s(T)$ values, and
16 from that distribution, we obtain the 95% confidence interval.

17

18 **5 Results and discussion**

19

20 **5.1 Ice nucleation efficiencies of plagioclase and alkali feldspars**

21 The values of $n_s(T)$ derived from the freezing experiments of the 15 feldspar samples are
22 shown in Figure 2 along with the $n_s(T)$ parameterisation from Atkinson et al. (2013) for BCS
23 376 microcline. The various groups of feldspars are indicated by colour which corresponds to
24 the regions of the phase diagram in Figure 1. We define potassium (K-) feldspars (red) as
25 those rich in K including microcline, orthoclase and sanidine; the Na end-member is albite
26 (green); and plagioclase series feldspars (blue) are a solid solution between albite and the
27 calcium end-member, anorthite.

28 Out of the six K-feldspars studied, five fall on or near the line defined by Atkinson et al.
29 (2013). These include three microcline samples and one sanidine sample, which have
30 different crystal structures. Sanidine has disordered Al atoms, microcline has ordered Al
31 atoms and orthoclase has intermediate order; these differences result in differences in



1 symmetry and hence space group. The freezing results indicate that Al disordering does not
2 play an important role in nucleation. However, one K-feldspar sample, TUD#3 microcline,
3 was substantially more active. This indicates that crystal structure and composition are not
4 the only factors dictating the ice nucleating ability of K-feldspars.

5 All plagioclase feldspars tested were less active ice nucleators than the K-feldspars which
6 were tested. There was relatively little variation in the ice nucleation activities of the
7 plagioclase solid solution series characterised by Carpenter (1986) and Carpenter et al.
8 (1985). For instance, of those feldspars that possess the plagioclase structure, greater sodium
9 content does not systematically increase effectiveness of ice nucleation. Overall, the results
10 for plagioclase feldspars indicate that they have an ice nucleating ability much smaller than
11 that of the K-feldspars.

12 It is also interesting to note that the ANC 68 synthetic anorthite had different nucleating
13 properties to the anorthite glass from which it was crystallised (and had the same
14 composition). The ANC 68 synthetic anorthite sample has a much more shallow $n_s(T)$ curve
15 than the glass. This is noteworthy, because the composition of these two materials is
16 identical, but the phase of the material is different. It demonstrates that crystallinity is not
17 required to cause nucleation, but the presence of crystallinity can provide rare sites which can
18 trigger nucleation at much warmer temperatures. In a future study it would be interesting to
19 attempt to probe the nature of these sites.

20 We tested three predominantly Na-feldspars (albite). Amelia albite was found to be highly
21 active, approaching that of TUD#3 microcline. The others, BCS 375 albite, and TUD#2 albite
22 were less active, intermediate between the K-feldspars and plagioclase feldspars.

23 To ensure that the high activity of Amelia albite and microcline TUD#3 was not caused by
24 contamination from biological INPs the samples were heated to 100°C in Milli-Q water for
25 15 minutes. This treatment will disrupt any protein based nucleators present (O'Sullivan et
26 al., 2015). No significant reduction in freezing temperatures (beyond what would be expected
27 from the activity decay described in Sect. 5.2) was observed suggesting that the highly active
28 INPs present are associated with the feldspars rather than biological contamination.

29 It has been noted by Vali (2014) that there is an indication that nucleators which are more
30 active at higher temperatures tend to have steeper slopes of $\ln J$ (nucleation rate) vs. We have
31 observed this trend here in the data shown in Figure 2 ($n_s(T)$ is proportional to J). The slopes



1 of experiments where freezing occurred at colder temperatures (plagioclases) generally being
2 flatter than those where freezing took place at warmer temperatures (alkali feldspars). Vali
3 (2014) suggests that this maybe the result of different observational methods. In this study we
4 have used a single method for all experiments so the trend is unlikely to be due to an
5 instrument artefact. The implication is that sites with lower activity tend to be more diverse in
6 nature. This may indicate that there are fewer possible ways to compose a site that is efficient
7 at nucleating ice and that there will be less variation in these sites as a result. The active sites
8 of lower activity may take a greater range of forms and so encompass a greater diversity of
9 activation temperatures.

10 To summarise, plagioclase feldspars tend to have relatively poor ice nucleating abilities, all
11 K-feldspars we tested are relatively good at nucleating ice and the albites are variable in their
12 nucleating activity. Out of the six K-feldspars tested, five have very similar activities and are
13 well approximated by the parameterisation of Atkinson et al. (2013) in the temperature- n_s
14 regime we investigated here. However, we have identified two alkali feldspar samples, one
15 K-feldspar and one albite, which are much more active than the others indicating that a factor
16 or factors other than the polymorph or composition determines the efficiency of alkali
17 feldspars as ice nucleators.

18 **5.2 The stability of active sites**

19 It was observed that the ice nucleation activity of ground Amelia albite and ground TUD #3
20 microcline declined over the course of ~30 minutes, the time between successive runs. Only
21 the initial run is shown in Figure 2 where the feldspar had spent only about 10 minutes in
22 suspension. This decay in activity over the course of ~30 mins was not seen in the other
23 feldspars. To investigate this effect samples of BCS 376 microcline, Amelia albite and TUD
24 #3 microcline were left in water within a sealed vial and tested at intervals over the course of
25 16 months, with a focus on the first 11 days. The results of these experiments are shown in
26 Figures 3 and 4. The median freezing temperature of the Amelia albite sample was most
27 sensitive to time spent in water, decreasing by 8 °C in 11 days and by 16 °C in 16 months.
28 The TUD#3 microcline sample decreased by about 2 °C in 16 months, but the freezing
29 temperatures of the BCS 376 did not change significantly over 16 months (within the
30 temperature uncertainty of $\pm 0.4^\circ\text{C}$). Clearly, the stability of the active sites responsible for ice
31 nucleation in these samples is highly variable.



1 Amelia albite is a particularly interesting case, where the highly active sites are also highly
2 unstable. For Amelia albite we observed that the ice nucleation ability of the powder directly
3 as supplied (the sample had been ground many years prior to experiments) was much lower
4 than the freshly ground sample. The n_s values for the ‘as-supplied’ Amelia albite are shown in
5 Figure 3. This suggests that the sites on Amelia albite are unstable and in general are
6 sensitive to the history of the sample. We note that from previous work that BCS 376 feldspar
7 ground to varied extents nucleates ice similarly (Whale et al., 2015a) and we have not
8 observed a decay of active sites of the BCS 376 microcline sample when stored in a dry vial
9 over the course of two years. It is also worth noting that freshly ground BCS 376 microcline
10 did not nucleate ice as efficiently as Amelia albite or TUD#3 microcline. These results
11 indicate that BCS 376 microcline contains very active sites, but that these sites are much
12 more stable than those found in Amelia albite.

13 It is evident that highly active sites in Amelia albite are generated by grinding but lose
14 activity when exposed to liquid water, and probably lose activity during exposure to
15 (presumably wet) air, returning to an activity level comparable to that of the plagioclase
16 feldspars. TUD#3 microcline also possesses a highly active site type sensitive to water
17 exposure but falls back to a level of activity higher than the other K-feldspars we have tested.
18 This second, less active site type is shown to be stable in water over the course of 16 months.
19 TUD#3 must possess populations of both more active, unstable sites and less active (although
20 still relatively active compared to the sites on other K-feldspars) stable sites. Amelia albite
21 possesses only unstable sites and much less active sites similar to those found on the
22 plagioclase feldspars we have tested.

23 These results indicate something of the nature of the active sites on feldspars. Throughout
24 this paper we refer to nucleation occurring on active sites, or specific sites, on the surface of
25 feldspar. It is thought that nucleation by most ice active minerals is consistent with nucleation
26 on active sites with a broad spectrum of activities (Herbert et al., 2014; Wheeler et al., 2015;
27 Niedermeier et al., 2015; Hiranuma et al., 2015; Wex et al., 2014; Augustin-Bauditz et al.,
28 2014; Niedermeier et al., 2010; Lüönd et al., 2010; Vali, 2014). However, the nature of these
29 sites is not known. It is postulated that active sites are related to defects in the structure and
30 therefore that each site has a characteristic nucleation ability, producing a spectrum of sites.
31 Defects are inherently less stable than the bulk of the crystal and we might expect these sites
32 to be affected by dissolution processes, or otherwise altered, in preference to the bulk of the
33 crystal (Parsons et al.;2015). The fact that we observe ice nucleation by populations of active



1 sites with different stabilities in water implies that these sites have different physical or
2 chemical characteristics. Furthermore, the fact that some populations of active sites are
3 sensitive to exposure to water suggests that the history of particles can be critical in
4 determining the ice nucleating ability of mineral dusts. This raises the question of whether
5 differences in ice nucleation efficiency observed by different instruments (Emersic et al.,
6 2015; Hiranuma et al., 2015), could be related to the different conditions particles experience
7 prior to nucleation.

8 **5.3 Comparison to literature data**

9 We have compared the $n_s(T)$ values for various feldspars from a range of literature sources
10 with data from this study in Figure 6. Inspection of this plot confirms that K-feldspars
11 nucleate ice more efficiently than the plagioclase feldspars. Also, with the exception of the
12 hyper-active Amelia albite sample, the K-feldspars are more active than the albites.

13 Results for BCS 376 microcline have been reported in several papers (Whale et al., 2015a;
14 Emersic et al., 2015; O'Sullivan et al., 2014; Atkinson et al., 2013). There is a discrepancy
15 between the cloud chamber data from Emersic et al. (2015) and the picolitre droplet cold
16 stage experiments at around -18°C , whereas the data at about -25°C are in agreement.
17 Emersic et al. (2015) attribute this discrepancy to aggregation of feldspar particles in
18 microlitre scale droplet freezing experiments reducing the surface area of feldspar exposed to
19 water leading to a lower $n_s(T)$ value. It is unlikely that this effect can account for the
20 discrepancy because in the temperature range of the Emersic et al. (2015) data the
21 comparison is being made to results from picolitre droplet freezing experiments which
22 Emersic et al. (2015) argue should not be affected by aggregation because there are not
23 enough particles present in each droplet to result in significant aggregation. Atkinson et al.
24 (2013) estimated that on average even the largest droplets only contained a few 10s of
25 particles. We also note that our microscope images of droplets show many individual
26 particles moving independently around in the picolitre droplets in those experiments,
27 indicating that the feldspar grains do not aggregate substantially. Hence, the discrepancy
28 between the data of Emersic et al. (2015) and Atkinson et al. (2013) at around -18°C cannot
29 be accounted for by aggregation. Furthermore, Atkinson et al. (2013) report that the surface
30 area determined from the laser diffraction size distribution of BCS 376 microcline in
31 suspension is 3.5 times smaller than that derived by the gas adsorption measurements (see
32 supplementary Figure 5 in Atkinson et al. (2013) and the corresponding discussion). This



1 difference in surface area can be accounted for by the fact that feldspar grains are not smooth
2 spheres, as assumed in the analysis of the laser diffraction data. Feldspar grains are well-
3 known to be rough and aspherical (Hodson et al., 1997). Atkinson et al. (2013) also note that
4 the laser diffraction technique lacks sensitivity to the smallest particles in the distribution
5 which will also lead to an underestimate in surface area. Nevertheless, the data presented by
6 Atkinson et al. (2013) suggests that aggregation of feldspar particles leading to reduced
7 surface area is at most a minor effect. As such the discrepancy between different instruments
8 remains unexplained and more work is needed on this topic.

9 Ice nucleation by single size-selected particles of TUD#1 microcline has been investigated by
10 Niedermeier et al. (2015) at temperatures below -23°C . We found that TUD#1 microcline
11 was in good agreement with K-feldspar parameterisation from Atkinson et al. (2013) between
12 about -6 and -11°C . Between -23 and -25°C , the $n_s(T)$ values produced by Niedermeier et al.
13 (2015) are similar (lower by a factor of roughly 4) to that of the Atkinson et al. (2013)
14 parameterisation, despite the different sample types. Niedermeier et al. (2015) used the
15 Leipzig Aerosol Cloud Interaction Simulator (LACIS), in which they size selected particles,
16 activated them to cloud droplets and then quantified the probability of freezing at a particular
17 temperature. It is interesting that the Niedermeier et al. (2015) $n_s(T)$ values curve off at
18 lower temperatures to a limiting value which they term n_s^* , indicating that nucleation by K-
19 feldspars may hit a maximum value and emphasises why we need to be cautious in
20 extrapolating $n_s(T)$ parameterisations beyond the range of experimental data.

21 The data for a microcline, a plagioclase (andesine) and albite from Zolles et al. (2015) is
22 consistent with our finding that plagioclase feldspars are less effective nucleators than K-
23 feldspars. It is also consistent with Atkinson et al. (2013) who found that albite is less
24 efficient at nucleating ice than microcline. However, the data for K-feldspar from Zolles et al.
25 (2015) sits below the line from Atkinson et al. (2013) for BCS 376 microcline and are lower
26 than the points from Niedermeier et al. (2015) for TUD#1 microcline. Their measurements
27 involved making up concentrated suspensions (19.6-4.8 wt%) suspensions and then creating a
28 water-in-oil emulsion where droplets were between 10-40 μm . They quote their particle sizes
29 as being between 1-10 μm for the feldspars. Atkinson et al. (2013) worked with 0.8 wt%
30 suspensions, with droplets of 9 to 19 μm where the mode particle size was ~ 700 nm. Hence,
31 Zolles et al. (2015) worked with a significantly more concentrated suspensions and larger
32 particles than used by Atkinson et al. (2013). However, it is not possible to determine
33 whether the observed difference in n_s is due to differences in the sample or the techniques



1 used, but may mean that certain K-feldspars nucleate ice less well than those defined by the
2 Atkinson et al. (2013) line in this temperature regime. This would be a very interesting result
3 as it may provide a point of difference that could provide insight into why K-feldspar
4 nucleate ice efficiently.

5 There has been relatively little work on what makes feldspar a good nucleator of ice. Zolles et
6 al. (2015) suggest that only K-feldspars will nucleate ice well on the basis that Ca^{2+} and Na^+
7 are chaotropic (structure breaking in water) while K^+ is kosmotropic (structure making in
8 water). We have only observed one feldspar that contains little K^+ but nucleates ice relatively
9 efficiently, Amelia albite. This feldspar loses its activity quickly in water and eventually
10 becomes more comparable to the plagioclase feldspars. It may be that the strong nucleation
11 observed is associated with the small amount of K^+ it contains and that once this dissolves
12 away the feldspar behaves like a plagioclase.

13 Augustin-Bauditz et al. (2014) tentatively concluded that microcline may nucleate ice more
14 efficiently than orthoclase at $n_s(T)$ values above about 10^6 cm^{-2} and at temperatures below -
15 23°C , the conditions where they performed their measurements. They arrived at this
16 conclusion by noting that NX-illite and Arizona test dust both contain orthoclase (8 and 20%,
17 respectively), but the $n_s(T)$ values they report for these materials are more than one order less
18 than microcline. In the microliter regimen this study we have observed some variability
19 amongst the K-feldspars (see Figure 2), but no difference between sanidine and the 4 out of 5
20 microclines which fall around the line defined by Atkinson et al. (2013). As discussed above,
21 the Al in sanidine is the least ordered, with microcline the most ordered and orthoclase at an
22 intermediate order, hence we observe no clear dependency on the ordering of Al in K-
23 feldspars. Further investigations of the ice nucleating ability of the various K-feldspar phases
24 at low temperature would be valuable. We could not do this in the present study with the
25 samples used here because we did not have sufficient quantities of the samples.

26

27 **6 Conclusions**

28 In this study we have analysed the ice nucleating ability of 15 well characterised feldspar
29 samples. These minerals include plagioclase feldspars (in the solid solution series between Ca
30 and Na end-members), the K-feldspars (sanidine, orthoclase and microcline) and albite (the
31 Na end-member). The results indicate that the alkali feldspars, including albite and K-



1 feldspars, tend to nucleate ice more efficiently than plagioclase feldspars. The plagioclase
2 feldspars nucleate ice at the lowest temperatures with no obvious dependence on the Ca-Na
3 ratio. The albites have a wide variety of nucleating abilities, with one sample nucleating ice
4 much more efficiently than the microcline sample Atkinson et al. (2013) studied. This hyper-
5 active albite lost its activity over time while suspended in water. Five out of six of the K-
6 feldspar samples we studied nucleated ice with a similar efficiency to the ‘generic’
7 microcline studied by Atkinson et al. (2013). A single K-feldspar we studied had a very high
8 activity, nucleating ice as warm as -2°C in our microliter droplet assay. The striking activity
9 of this hyperactive microcline decayed with time spent in water, but not to the same extent as
10 the hyper-active albite sample. While the hyperactive sites are sensitive, to varying degrees,
11 to time spent in water, the activity of the ‘generic’ microcline sample used by Atkinson et al.
12 (Atkinson et al., 2013) did not change significantly.

13 In light of these findings, we suggest that there are at least three classes of site present in the
14 feldspars studied here: i) relatively inactive sites associated with plagioclase feldspars; ii)
15 more active sites associated with K-feldspars that is stable in water over the course of many
16 months; iii) hyper-active sites associated with one albite and one K-feldspar that we studied
17 that loses activity when exposed to water.

18 The specific details of these active sites continue to elude us, although it appears that they are
19 only present in alkali feldspars and in particular, the K-feldspars. Unlike the plagioclase
20 feldspars which form a solid solution, the Na and K feldspars in alkali feldspars are often
21 exsolved, possessing intergrowths of the Na and K feldspars referred to as microtexture
22 (Parsons et al., 2015). It is possible that the boundaries between the two phases in the
23 intergrowth provide sites for nucleation that are not present in plagioclase feldspars. More
24 work is needed to explore this possibility.

25 In a previous study Atkinson et al. (2013) used an $n_s(T)$ parameterisation of a single K-
26 feldspar (BCS 376 microcline) to approximate the ice nucleating properties of desert dust in a
27 global aerosol model. Given that four out of five of the K-feldspars we studied here have very
28 similar ice nucleating abilities, this approximation seems reasonable. However, we have
29 identified two hyper-active feldspars and do not know how representative these samples are
30 of natural feldspars in dust emission regions. We also note that the active sites on these
31 feldspars are less stable than those of BCS 376 microcline. Nevertheless, there is the



1 possibility that the parameterisation used by Atkinson et al. (2013) underestimates the
2 contribution of feldspars at warmer temperatures above about -15°C .
3 In the longer term it may be possible to identify what it is that leads to the variation in ice
4 nucleation activity between the different feldspar classes. In particular, the nature of the
5 active sites in the hyper-active feldspars and the reason plagioclase is so much poorer at
6 nucleating ice are subjects of interest. The instability of the sites in the hyperactive feldspars
7 may be related to dissolution of feldspar in water and investigation of this process may allow
8 progress towards understanding of nucleation by feldspars. The results presented here are
9 empirical in nature and do not provide a thorough underpinning understanding of the nature
10 of the active sites. Nevertheless, the fact that the feldspar group of minerals have vastly
11 different ice nucleating properties despite possessing very similar crystal structures may
12 provide us with a means of gaining a fundamental insight to heterogeneous ice nucleation.

13
14

15 **Acknowledgments**

16 We would like to acknowledge Theodore Wilson and Alexei Kiselev for helpful discussions
17 and John Morris for introducing TFW and MAC. We are grateful to Alexei Kiselev and
18 Martin Ebert for providing the TUD samples. Alex Harrison thanks the School of Earth and
19 Environment for an Undergraduate Research Scholarship which allowed him to make many
20 of the measurements presented in this paper. We would like to thank the National
21 Environmental Research Council, (NERC, NE/I013466/1; NE/I020059/1; NE/K004417/1;
22 NE/I019057/1; NE/M010473/1) the European Research Council (ERC, 240449 ICE; 632272
23 IceControl; 648661 MarineIce), and the Engineering and Physical Sciences Research Council
24 (EPSRC, EP/M003027/1) for funding.

25
26

27 Atkinson, J. D., Murray, B. J., Woodhouse, M. T., Whale, T. F., Baustian, K. J., Carslaw, K. S., Dobbie,
28 S., O'Sullivan, D., and Malkin, T. L.: The importance of feldspar for ice nucleation by mineral dust in
29 mixed-phase clouds, *Nature*, 498, 355-358, 10.1038/nature12278, 2013.

30



- 1 Augustin-Bauditz, S., Wex, H., Kanter, S., Ebert, M., Niedermeier, D., Stolz, F., Prager, A., and
2 Stratmann, F.: The immersion mode ice nucleation behavior of mineral dusts: A comparison of
3 different pure and surface modified dusts, *Geophys. Res. Lett.*, 41, 7375-7382,
4 10.1002/2014gl061317, 2014.
5
- 6 Carpenter, M.: Experimental delineation of the “e” \rightleftharpoons i\bar{1} and “e” \rightleftharpoons c\bar{1} transformations in
7 intermediate plagioclase feldspars, *Phys. Chem. Minerals.*, 13, 119-139, 10.1007/bf00311902, 1986.
8
- 9 Carpenter, M. A., McConnell, J. D. C., and Navrotsky, A.: Enthalpies of ordering in the plagioclase
10 feldspar solid solution, *Geochim. Cosmochim. Acta*, 49, 947-966, [http://dx.doi.org/10.1016/0016-](http://dx.doi.org/10.1016/0016-7037(85)90310-2)
11 7037(85)90310-2, 1985.
12
- 13 Carpenter, M. A.: Mechanisms and kinetics of al-si ordering in anorthite; I, Incommensurate
14 structure and domain coarsening, *Am. Mineral.*, 76, 1110-1119, 1991.
15
- 16 Connolly, P. J., Möhler, O., Field, P. R., Saathoff, H., Burgess, R., Choulaton, T., and Gallagher, M.:
17 Studies of heterogeneous freezing by three different desert dust samples, *Atmos. Chem. Phys.*, 9,
18 2805-2824, 10.5194/acp-9-2805-2009, 2009.
19
- 20 Cox, S. J., Kathmann, S. M., Purton, J. A., Gillan, M. J., and Michaelides, A.: Non-hexagonal ice at
21 hexagonal surfaces: The role of lattice mismatch, *Phys. Chem. Chem. Phys.*, 14, 7944-7949,
22 10.1039/c2cp23438f, 2012.
23
- 24 Cox, S. J., Kathmann, S. M., Slater, B., and Michaelides, A.: Molecular simulations of heterogeneous
25 ice nucleation. I. Controlling ice nucleation through surface hydrophilicity, *J. Chem. Phys.*, 142,
26 184704, doi:<http://dx.doi.org/10.1063/1.4919714>, 2015a.
27
- 28 Cox, S. J., Kathmann, S. M., Slater, B., and Michaelides, A.: Molecular simulations of heterogeneous
29 ice nucleation. II. Peeling back the layers, *J. Chem. Phys.*, 142, 184705,
30 doi:<http://dx.doi.org/10.1063/1.4919715>, 2015b.
31
- 32 Deer, W. A., Howie, R. A., and Zussman, J.: An introduction to the rock forming minerals, 2nd ed.,
33 Addison Wesley Longman, Harlow, UK, 1992.
34
- 35 DeMott, P. J., Sassen, K., Poellot, M. R., Baumgardner, D., Rogers, D. C., Brooks, S. D., Prenni, A. J.,
36 and Kreidenweis, S. M.: African dust aerosols as atmospheric ice nuclei, *Geophys. Res. Lett.*, 30,
37 1732, 10.1029/2003GL017410, 2003.
38
- 39 Emersic, C., Connolly, P. J., Boulton, S., Campana, M., and Li, Z.: Investigating the discrepancy between
40 wet-suspension- and dry-dispersion-derived ice nucleation efficiency of mineral particles, *Atmos.*
41 *Chem. Phys.*, 15, 11311-11326, 10.5194/acp-15-11311-2015, 2015.
42



- 1 Fitzner, M., Sosso, G. C., Cox, S. J., and Michaelides, A.: The many faces of heterogeneous ice
2 nucleation: Interplay between surface morphology and hydrophobicity, *J. Am. Chem. Soc.*, 137,
3 13658-13669, 10.1021/jacs.5b08748, 2015.
4
- 5 Freedman, M. A.: Potential sites for ice nucleation on aluminosilicate clay minerals and related
6 materials, *J. Phys. Chem. Lett.*, 6, 3850-3858, 10.1021/acs.jpcclett.5b01326, 2015.
7
- 8 Ginoux, P., Prospero, J. M., Gill, T. E., Hsu, N. C., and Zhao, M.: Global-scale attribution of
9 anthropogenic and natural dust sources and their emission rates based on modis deep blue aerosol
10 products, *Rev. Geophys.*, 50, RG3005, 10.1029/2012rg000388, 2012.
11
- 12 Herbert, R. J., Murray, B. J., Whale, T. F., Dobbie, S. J., and Atkinson, J. D.: Representing time-
13 dependent freezing behaviour in immersion mode ice nucleation, *Atmos. Chem. Phys.*, 14, 8501-
14 8520, 10.5194/acp-14-8501-2014, 2014.
15
- 16 Herbert, R. J., Murray, B. J., Dobbie, S. J., and Koop, T.: Sensitivity of liquid clouds to homogenous
17 freezing parameterizations, *Geophys. Res. Lett.*, 42, 1599-1605, 10.1002/2014gl062729, 2015.
18
- 19 Hiranuma, N., Augustin-Bauditz, S., Bingemer, H., Budke, C., Curtius, J., Danielczok, A., Diehl, K.,
20 Dreischmeier, K., Ebert, M., Frank, F., Hoffmann, N., Kandler, K., Kiselev, A., Koop, T., Leisner, T.,
21 Möhler, O., Nillius, B., Peckhaus, A., Rose, D., Weinbruch, S., Wex, H., Boose, Y., DeMott, P. J., Hader,
22 J. D., Hill, T. C. J., Kanji, Z. A., Kulkarni, G., Levin, E. J. T., McCluskey, C. S., Murakami, M., Murray, B. J.,
23 Niedermeier, D., Petters, M. D., O'Sullivan, D., Saito, A., Schill, G. P., Tajiri, T., Tolbert, M. A., Welti,
24 A., Whale, T. F., Wright, T. P., and Yamashita, K.: A comprehensive laboratory study on the
25 immersion freezing behavior of illite nx particles: A comparison of 17 ice nucleation measurement
26 techniques, *Atmos. Chem. Phys.*, 15, 2489-2518, 10.5194/acp-15-2489-2015, 2015.
27
- 28 Hodson, M. E., Lee, M. R., and Parsons, I.: Origins of the surface roughness of unweathered alkali
29 feldspar grains, *Geochim. Cosmochim. Acta*, 61, 3885-3896, 10.1016/s0016-7037(97)00197-x, 1997.
30
- 31 Hoose, C., Lohmann, U., Erdin, R., and Tegen, I.: The global influence of dust mineralogical
32 composition on heterogeneous ice nucleation in mixed-phase clouds, *Environ. Res. Lett.*, 3,
33 10.1088/1748-9326/3/2/025003, 2008.
34
- 35 Hoose, C., Kristjánsson, J. E., Chen, J.-P., and Hazra, A.: A classical-theory-based parameterization of
36 heterogeneous ice nucleation by mineral dust, soot, and biological particles in a global climate
37 model, *J. Atmos. Sci.*, 67, 2483-2503, 10.1175/2010jas3425.1, 2010.
38
- 39 Hoose, C., and Möhler, O.: Heterogeneous ice nucleation on atmospheric aerosols: A review of
40 results from laboratory experiments, *Atmos. Chem. Phys.*, 12, 9817-9854, 10.5194/acp-12-9817-
41 2012, 2012.
42
- 43 Hu, X. L., and Michaelides, A.: Ice formation on kaolinite: Lattice match or amphoterism?, *Surf. Sci.*,
44 601, 5378-5381, 10.1016/j.susc.2007.09.012, 2007.



1

2 Löönd, F., Stetzer, O., Welti, A., and Lohmann, U.: Experimental study on the ice nucleation ability of
3 size-selected kaolinite particles in the immersion mode, *J. Geophys. Res.*, 115, D14201,
4 10.1029/2009jd012959, 2010.

5

6 Lupi, L., Hudait, A., and Molinero, V.: Heterogeneous nucleation of ice on carbon surfaces, *J. Am.*
7 *Chem. Soc.*, 136, 3156-3164, 10.1021/ja411507a, 2014.

8

9 Lupi, L., and Molinero, V.: Does hydrophilicity of carbon particles improve their ice nucleation
10 ability?, *J. Phys. Chem. A*, 118, 7330-7337, 10.1021/jp4118375, 2014.

11

12 Murray, B. J., O'Sullivan, D., Atkinson, J. D., and Webb, M. E.: Ice nucleation by particles immersed in
13 supercooled cloud droplets, *Chem. Soc. Rev.*, 41, 6519-6554, 10.1039/C2CS35200A, 2012.

14

15 Niedermeier, D., Hartmann, S., Shaw, R. A., Covert, D., Mentel, T. F., Schneider, J., Poulain, L., Reitz,
16 P., Spindler, C., Clauss, T., Kiselev, A., Hallbauer, E., Wex, H., Mildenerger, K., and Stratmann, F.:
17 Heterogeneous freezing of droplets with immersed mineral dust particles - measurements and
18 parameterization, *Atmos. Chem. Phys.*, 10, 3601-3614, 10.5194/acp-10-3601-2010, 2010.

19

20 Niedermeier, D., Augustin-Bauditz, S., Hartmann, S., Wex, H., Ignatius, K., and Stratmann, F.: Can we
21 define an asymptotic value for the ice active surface site density for heterogeneous ice nucleation?,
22 *J. Geophys. Res.: Atmos.*, 120, 5036-5046, 10.1002/2014jd022814, 2015.

23

24 Niemand, M., Möhler, O., Vogel, B., Vogel, H., Hoose, C., Connolly, P., Klein, H., Bingemer, H.,
25 DeMott, P. J., Skrotzki, J., and Leisner, T.: A particle-surface-area-based parameterization of
26 immersion freezing on desert dust particles, *J. Atmos. Sci.*, 69, 10.1175/jas-d-11-0249.1, 2012.

27

28 O'Sullivan, D., Murray, B. J., Malkin, T. L., Whale, T. F., Umo, N. S., Atkinson, J. D., Price, H. C.,
29 Baustian, K. J., Browse, J., and Webb, M. E.: Ice nucleation by fertile soil dusts: Relative importance
30 of mineral and biogenic components, *Atmos. Chem. Phys.*, 14, 1853-1867, 10.5194/acp-14-1853-
31 2014, 2014.

32

33 O' Sullivan, D., Murray, B. J., Ross, J. F., Whale, T. F., Price, H. C., Atkinson, J. D., Umo, N. S., and
34 Webb, M. E.: The relevance of nanoscale biological fragments for ice nucleation in clouds, *Sci. Rep.*,
35 5, 10.1038/srep08082, 2015.

36

37 Parsons, I., Fitz Gerald, J. D., and Lee, M. R.: Routine characterization and interpretation of complex
38 alkali feldspar intergrowths, *Am. Mineral.*, 100, 1277-1303, 10.2138/am-2015-5094, 2015.

39

40 Reinhardt, A., and Doye, J. P. K.: Effects of surface interactions on heterogeneous ice nucleation for a
41 monatomic water model, *J. Chem. Phys.*, 141, 10.1063/1.4892804, 2014.

42



- 1 Riechers, B., Wittbracht, F., Hütten, A., and Koop, T.: The homogeneous ice nucleation rate of water
2 droplets produced in a microfluidic device and the role of temperature uncertainty, *Phys. Chem.*
3 *Chem. Phys.*, 15, 5873-5887, 10.1039/C3CP42437E, 2013.
4
- 5 Slater, B., Michaelides, A., Salzmann, C. G., and Lohmann, U.: A blue-sky approach to understanding
6 cloud formation, *B. Am. Meteorol. Soc.*, 10.1175/bams-d-15-00131.1, 2015.
7
- 8 Umo, N. S., Murray, B. J., Baeza-Romero, M. T., Jones, J. M., Lea-Langton, A. R., Malkin, T. L.,
9 O'Sullivan, D., Neve, L., Plane, J. M. C., and Williams, A.: Ice nucleation by combustion ash particles at
10 conditions relevant to mixed-phase clouds, *Atmos. Chem. Phys.*, 15, 5195-5210, 10.5194/acp-15-
11 5195-2015, 2015.
12
- 13 Vali, G.: Interpretation of freezing nucleation experiments: Singular and stochastic; sites and
14 surfaces, *Atmos. Chem. Phys.*, 14, 5271-5294, 10.5194/acp-14-5271-2014, 2014.
15
- 16 Wenk, H.-R., and Bulakh, A.: *Minerals: Their constitution and origin*, Cambridge University Press,
17 Cambridge, UK, 2004.
18
- 19 Wex, H., DeMott, P. J., Tobo, Y., Hartmann, S., Rösch, M., Clauss, T., Tomsche, L., Niedermeier, D.,
20 and Stratmann, F.: Kaolinite particles as ice nuclei: Learning from the use of different kaolinite
21 samples and different coatings, *Atmos. Chem. Phys.*, 14, 5529-5546, 10.5194/acp-14-5529-2014,
22 2014.
23
- 24 Whale, T. F., Murray, B. J., O'Sullivan, D., Wilson, T. W., Umo, N. S., Baustian, K. J., Atkinson, J. D.,
25 Workneh, D. A., and Morris, G. J.: A technique for quantifying heterogeneous ice nucleation in
26 microlitre supercooled water droplets, *Atmos. Meas. Tech.*, 8, 2437-2447, 10.5194/amt-8-2437-
27 2015, 2015a.
28
- 29 Whale, T. F., Rosillo-Lopez, M., Murray, B. J., and Salzmann, C. G.: Ice nucleation properties of
30 oxidized carbon nanomaterials, *J. Phy. Chem. Lett.*, 3012-3016, 10.1021/acs.jpcllett.5b01096, 2015b.
31
- 32 Wheeler, M. J., Mason, R. H., Steunenberg, K., Wagstaff, M., Chou, C., and Bertram, A. K.: Immersion
33 freezing of supermicron mineral dust particles: Freezing results, testing different schemes for
34 describing ice nucleation, and ice nucleation active site densities, *J. Phys. Chem. A*, 119, 4358-4372,
35 10.1021/jp507875q, 2015.
36
- 37 Wilson, T. W., Ladino, L. A., Alpert, P. A., Breckels, M. N., Brooks, I. M., Browse, J., Burrows, S. M.,
38 Carslaw, K. S., Huffman, J. A., Judd, C., Kilitau, W. P., Mason, R. H., McFiggans, G., Miller, L. A.,
39 Najera, J. J., Polishchuk, E., Rae, S., Schiller, C. L., Si, M., Temprado, J. V., Whale, T. F., Wong, J. P. S.,
40 Wurl, O., Yakobi-Hancock, J. D., Abbatt, J. P. D., Aller, J. Y., Bertram, A. K., Knopf, D. A., and Murray,
41 B. J.: A marine biogenic source of atmospheric ice-nucleating particles, *Nature*, 525, 234-238,
42 10.1038/nature14986, 2015.
43
- 44 Wittke, W., and Sykes, R.: *Rock mechanics*, Springer Berlin, 1990.



1

2 Zielke, S. A., Bertram, A. K., and Patey, G. N.: Simulations of ice nucleation by kaolinite (001) with
3 rigid and flexible surfaces, *J. Phys. Chem. B*, 10.1021/acs.jpccb.5b09052, 2015.

4

5 Zolles, T., Burkart, J., Häusler, T., Pummer, B., Hitzemberger, R., and Grothe, H.: Identification of ice
6 nucleation active sites on feldspar dust particles, *J. Phys. Chem. A*, 119, 2692-2700,
7 10.1021/jp509839x, 2015.

8

9

10

11

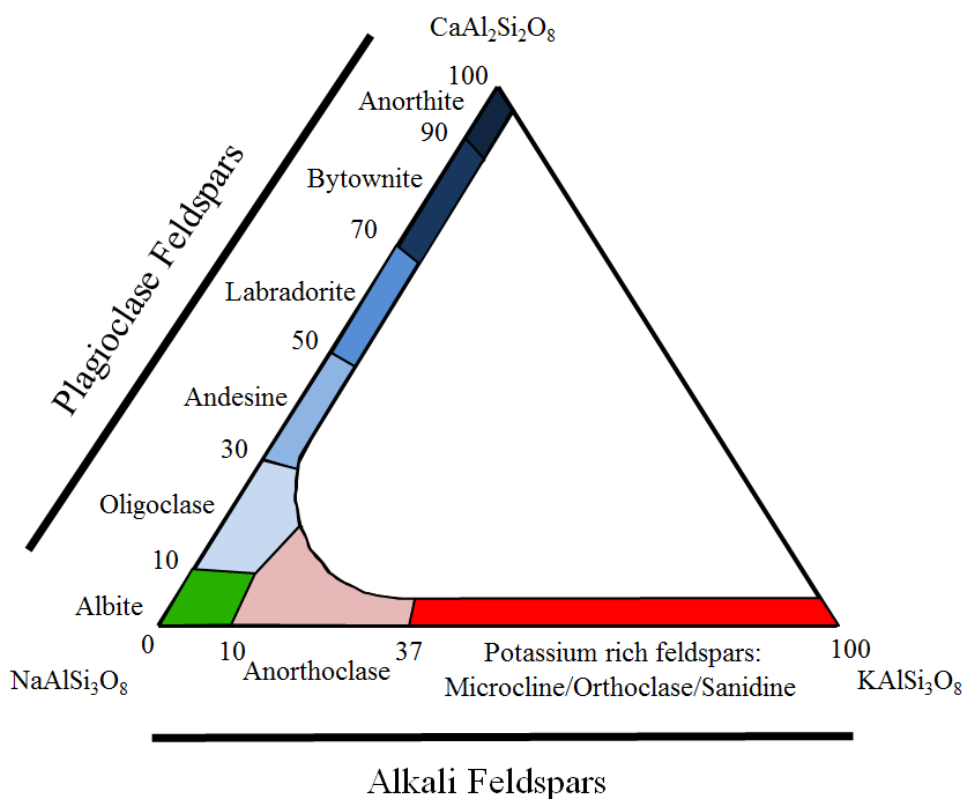
12

13

14

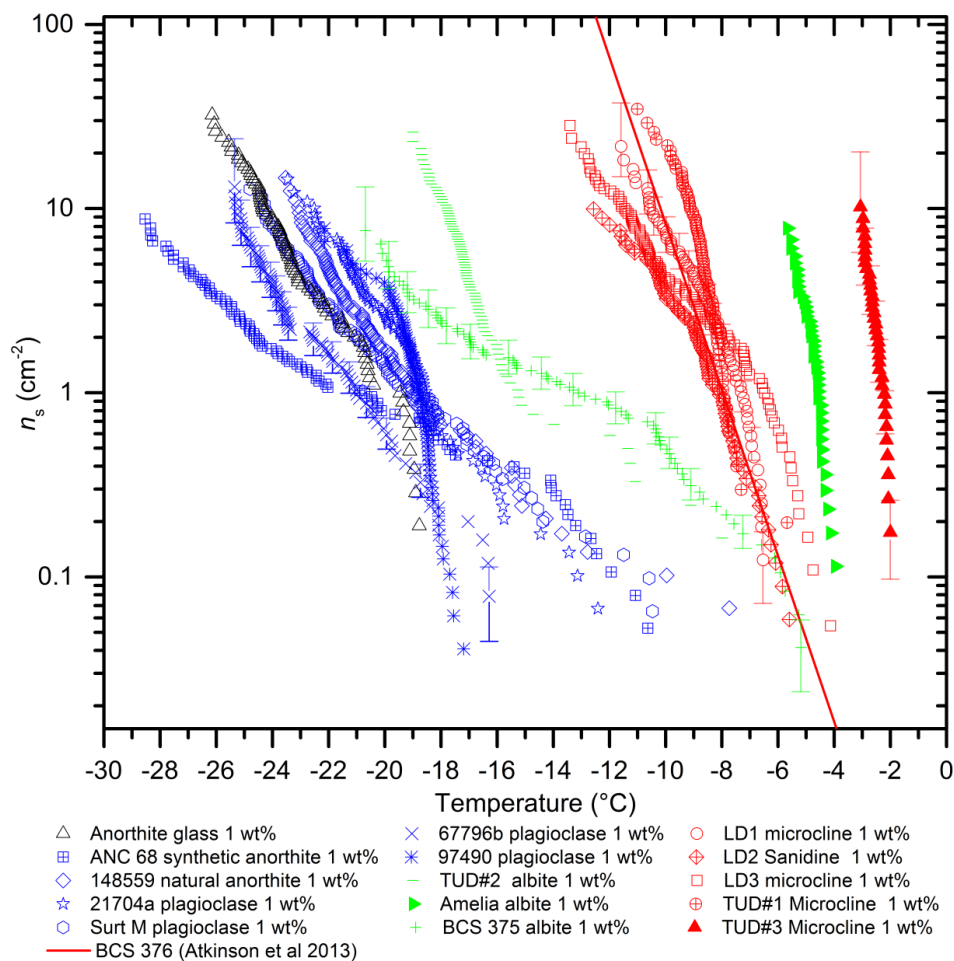
15

16



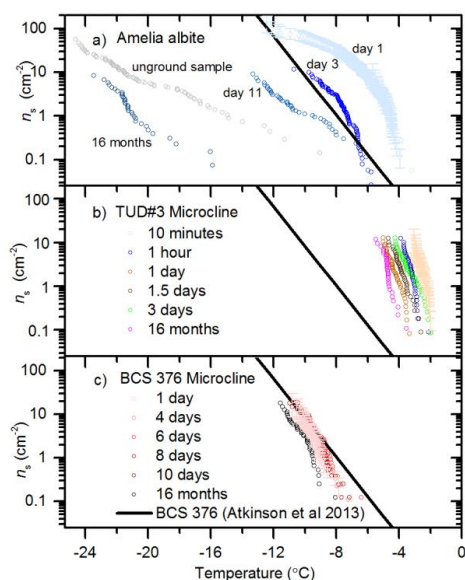
1
2
3
4

Figure 1: The ternary composition diagram for the feldspars group based on similar figures in the literature (Wittke and Sykes, 1990; Deer et al., 1992).



1

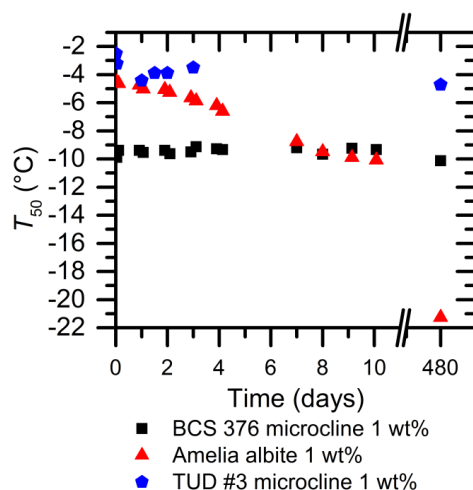
2 Figure 2: Ice nucleation efficiency expressed as $n_s(T)$ for the various feldspars tested in this
 3 study. The K-feldspars are coloured red, the plagioclase feldspars are coloured blue, the
 4 albites are coloured green and the feldspar glass is coloured black. Except for Amelia albite
 5 and TUD#1 microcline all samples were tested twice and the data from the two runs
 6 combined. Sample information can be found in tables 1 and 2. Temperature uncertainty is
 7 $\pm 0.4^{\circ}\text{C}$. Y-Error bars calculated using the Poisson Monte Carlo procedure described in Sect.
 8 4. Data points with large uncertainties greater than an order of magnitude have been removed,
 9 these are invariably the first one or two freezing events of a given experiment. For clarity
 10 error bars have only been included on a selection of datasets (TUD#3 microcline, LD1
 11 microcline, BCS 375 albite and 67796b plagioclase). The error bars shown are typical.
 12 Background subtraction of the type conducted by O'Sullivan et al. (2015) made insignificant
 13 difference to the reported $n_s(T)$ values.



1

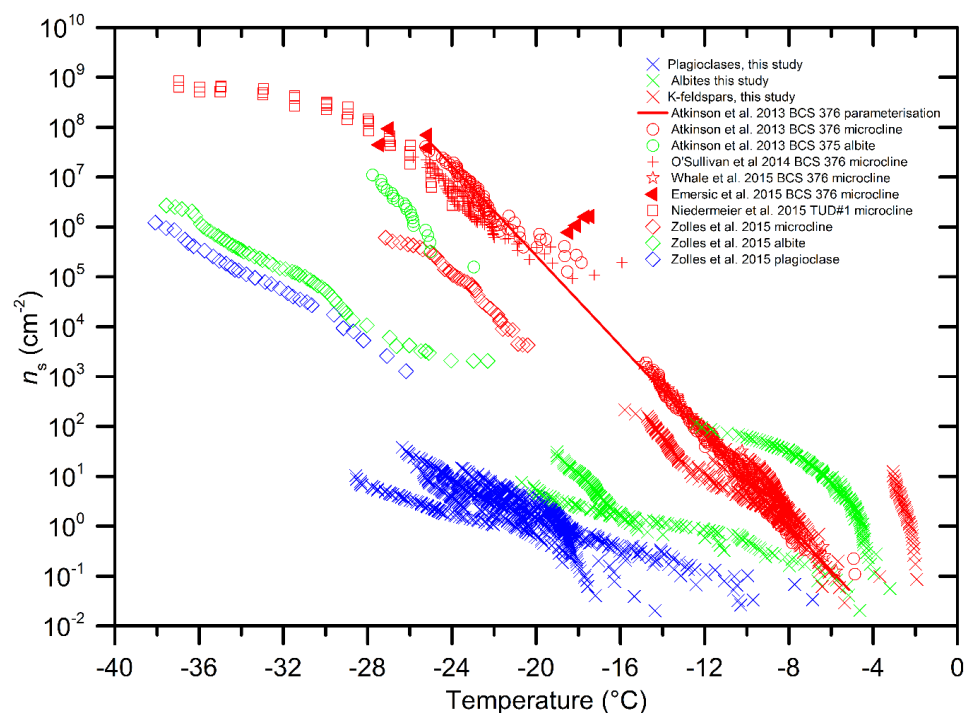
2 Figure 3: The dependence of n_s on time spent in water for three feldspar samples. The time
 3 periods indicate how long samples were left in contact with water. Fresh samples were tested
 4 minutes after preparation of suspensions. Note that ice nucleation temperatures of BCS 376
 5 are almost the same after 16 months in water while those of Amelia albite decreases by
 6 around 16°C. TUD #3 microcline loses activity quickly in the first couple of days of exposure
 7 to water but total decrease in nucleation temperatures after 16 months is only around 2°C.

8



9

10 Figure 4: Median freezing temperature against time left in suspension for BCS 376
 11 microcline, TUD#3 microcline and Amelia albite.



1

2 Figure 5: Comparison of literature data from Atkinson et al. (2013), Emersic et al. (2015),
3 Niedermeier et al. (2015) and Zolles et al. (2015) with data from this study. Feldspars are
4 coloured according to their composition, as in Figure 2. 0.1 wt% data for Amelia albite and
5 LD1 microcline, which is not shown in figure 2, has been included. Where samples are
6 known to lose activity with time the most active runs have been shown. Note that data from
7 Niedermeier et al. (2015) includes some data from Augustin-Bauditz et al. (2014).

8

9

10

11

12

13

14

15

16

17



1 Table 1. Plagioclase feldspars used in this study.

Sample	BET Surface area (m ² /g)	Composition*	Source of composition/phase data
Anorthite glass	1.18 ± 0.01 m ² /g	An ₁₀₀	(Carpenter, 1991)
ANC 68	4.25 ± 0.02 m ² /g	An ₁₀₀	(Carpenter, 1991) describes similar feldspars
148559	3.07 ± 0.02 m ² /g	An _{99.5} Ab _{0.5}	-----
21704a	3.07 ± 0.03 m ² /g	An ₈₆ Ab ₁₄	(Carpenter et al., 1985)
Surt M	3.00 ± 0.05 m ² /g	An ₆₄ Ab ₃₆	(Carpenter, 1986)
67796b	2.80 ± 0.03 m ² /g	An ₆₀ Or ₁ Ab ₃₉	(Carpenter et al., 1985)
97490	5.63 ± 0.03 m ² /g	An ₂₇ Or ₁ Ab ₇₁	(Carpenter et al., 1985)

2 *This refers to the chemical makeup of the feldspars. An stands for anorthite, the calcium end-
 3 member, Ab stands for albite, the sodium end-member and Or stands for orthoclase, the potassium
 4 end-member.

5 Table 2. Alkali feldspars used in this study.

Sample	BET Surface area (m ² /g)	Dominant feldspar phase	Source of composition/phase data
LD1 microcline	1.99 ± 0.05 m ² /g	microcline	XRD
LD2 sanidine	3.77 ± 0.03 m ² /g	sanidine	XRD
LD3 microcline	1.78 ± 0.01 m ² /g	microcline	XRD
BCS 376 microcline	2.03 ± 0.01 m ² /g	microcline	Reference sample/XRD (Atkinson et al., 2013)
Amelia Albite (un-ground)	0.73 ± 0.02 m ² /g	albite	(Carpenter et al., 1985)
Amelia Albite ground	3.94 ± 0.02 m ² /g	albite	(Carpenter et al., 1985)
TUD#1 microcline	1.23 ± 0.03 m ² /g	microcline	XRD
TUD#2 albite	1.39 ± 0.03 m ² /g	albite*	XRD
TUD#3 microcline	2.84 ± 0.03 m ² /g	microcline	XRD
BCS 375 albite	5.8 ± 0.03 m ² /g	albite	Reference sample/XRD (Atkinson et al., 2013)

6 * We note that the XRD pattern was also consistent with oligoclase, which is close to albite in
 7 composition. The identification of albite is consistent with that of Alexei Kiselev (Personal
 8 communication).

9